Materials Physics and Mechanics 46 (2020) 122-131 Received: November 30, 2020

SYNTHESIS OF METALLIC COMPOSITE BASED ON IRON FRAME AND SiC NANOSTRUCTURES AND ITS STRENGTH PROPERTIES

E.G. Zemtsova, D.V. Yurchuk, Yu.V. Sidorov, B.N. Semenov*, N.F. Morozov, V.M. Smirnov

St Petersburg State University, Universitetskaya emb. 7/9, St Petersburg 199034, Russia

*e-mail: b.semenov@spbu.ru

Abstract. The article discusses a new approach to the synthesis of metallic composite materials based on nanostructuring of a metal frame (on the example of iron) by SiC nanostructures (10-50 nm). Optimal conditions are established for the nano-SiC coating on the porous Fe surface during sequential chemisorption of $Cl_2Si(CH_3)_2$ and CH_4 molecules from the gas phase. The resulting composite possesses enhanced strength in comparison with the best steel samples although the residual porosity (up to 5%) of Fe matrix is still preserved after pressing.

Keywords: composite, metallic framework, iron, disperse phase, SiC, ultimate strength

1. Introduction

One of the crucial tasks of modern materials science is the development of new composites with improved functional properties [1]. The importance of an interdisciplinary approach to this task should be noted [2-4]. The structural organization of matter is one of the key problems of natural science. This is because the questions of the matter organization at different levels are studied by physics, mechanics, chemistry, and biology. Establishing physical and chemical parameters that control the properties of artificially ordered nanostructures materials based on them is one of the most important areas of world research. From the physical mesomechanics point of view, chemical nanostructuring of materials leads to new objects with multi-level organization, which is necessary for a more correct approach to the study (experimental and theoretical) of structural transformation at the nanoscale level [2-6].

Iron- or aluminum-based composites are important materials for a wide range of structural applications. An enhancement of the mechanical properties of iron- or aluminum-based composites can be realized by creating a nanoscale structure with high uniformity and well-formed intergranular boundaries [2,7].

Known metal composites fabrication techniques [1,2] cannot give a uniform distribution of the dispersed phase in the bulk matrix. The lack of uniform distribution prevents the achievement of the maximal mechanical properties of the composite [6].

We have developed a new approach to the synthesis of composites based on the processes of three-dimensional nanostructuring (reinforcement) of the matrix frame with a dispersed nanophase [8-11].

Metal matrix nanostructuring involves the distribution of nano-carbide in the bulk porous matrix. The product is a composite material comprising an iron metallic frame reinforced (permeated) with silicon carbide (SiC)-based nanostructures with improved strength.

http://dx.doi.org/10.18720/MPM.4612020_12

The purpose of this work was to establish the conditions for obtaining SiC nanolayers on the nanodispersed porous Fe powder surface. In fact, the composite formation process includes 3 main stages:

1. Fabrication of Fe matrix with a pre-defined porosity;
2. Surface modification of prepared porous Fe matrix with SiC (10-50 nm) nanostructures.
3. Pressing and sintering to produce a massive (non-porous) Fe/SiC nanocomposite.

2. Materials and Methods

Chemicals. The chemicals were obtained from commercial suppliers: $SiCl_4$ (99,6%), (Alfa Aesar), CCl_4, $Cl_2Si(CH_3)_2$. (Sigma-Aldrich), $FeCl_2 \cdot 4H_2O$, NaOH (Merck), and CH_4 (gaseous) (Lengaz).

Methods. The powder phases were identified by powder XRD using Bruker D2 Phaser diffractometer with a cobalt anode.

The morphology of samples was studied with the scanning electron microscope (Zeiss Merlin) operated at 10–15 kV in In-lens, SE2, and EDS modes. The magnifications from 300 up to 600 000 (spatial resolution 1 nm) were used.

The Mössbauer spectra were recorded at the constant acceleration in combination with the use of a multichannel Nuclear Data Instruments ND 60 analyzer. In our work, we used a ^{57}Co radiation source that decays to ^{57}Fe.

Specific surface (S_{sp}) of the samples were determined using BET model of nitrogen adsorption. From specific surface values S_{sp}, the average size of powder particles can be evaluated according to the equation $d_{av} = 6/(\rho\ S)$, where ρ is substance density.

The ultimate strength (σ_b) was determined on the AG-50kNXD desktop testing machine (Shimadzu) at the Resource Center for innovative composite materials technologies of St. Petersburg State University.

Iron nanoparticles fabrication. As it is known, with a decrease in grain size, the strength increases while maintaining plasticity. The effect of low-temperature and high-speed superplasticity is manifested, and physical properties changes are observed.

In order to obtain Fe NPs of high dispersion, it is necessary to use the precursors that could be reduced at a possibly lower temperature [1]. So, we selected the way via amorphous iron oxide-hydroxide FeOOH as intermediate.

FeOOH was synthesized by precipitation from $FeSO_4 \cdot 7H_2O$ using NaOH in distilled water.

Final precipitate washed with distilled water and dried at 120°C for 5 h.

Fe nanopowders were obtained by subsequent FeOOH (1 g) reduction in a quartz tube furnace with nichrome heaters at 400°C for 90 min. Hydrogen (≥99.99% pure) was used as the reductant. The rate of the H_2 supply was $2–5 \cdot 10^{-6}$ m^3/s. As a result, we produced Fe nanoparticles denoted as $[Fe]_aH$.

Iron nanoparticles compaction. $[Fe]_aH$ (particle size of 60 nm) was uniaxially compacted in a cylindrical mold (internal diameter 15 mm; the height of the compact 5-7 mm).

Optimized pressing conditions were suggested after pre-experiments: powder weight 9g, height of the resulting sample h = 4.96 mm, diameter = 15 mm, ρ = 4.60 g/ml. The pressure of 200 MPa loaded during 60 s, maintained for 180 s, then unloaded during 30 s.

The compacts' density was determined by hydrostatic weighing with an accuracy of 2 %.

These conditions provide Fe samples with 20-30% residual porosity. This is proved to be sufficient for further surface chemical reactions.

ALD deposition of SiC. SiC dispersed phase on Fe was produced by ALD [12-18] in a flow-type reactor. The ALD technique is based on alternating chemical reactions of low molecular weight reagents on the surface. As a result of each reaction cycle, new carbide unit was added chemically bonded to the support. Depending on the number of such cycles, layers of the various thickness are synthesized. The chemical composition of the samples was determined by photocolorimetry for silicon and chemical analysis for carbon, based on burning the sample in oxygen and gas chromatographic determination of carbon in CO and CO_2.

Stream of dry helium was used both to provide an inert atmosphere and to assist the removal of gaseous by-products from the reactor. The synthesis temperature was 200-500°C.

It's important that when storing, $[Fe]_aH$ is covered by the surface oxide layer of varying thickness. The composition of the oxide layer (usually 3-5 nm thick) is not stable and varies depending on storage conditions and other factors. So, it was necessary to purify Fe surface from the oxide layer before deposition. For this purpose, we used surface standardization. According to the developed approach, at this stage, metallic Fe particles were chlorinated to form ═Fe-Cl groups on the surface:

$[Fe]_aH + CCl_4 \rightarrow [Fe]_a–Cl + HCl\uparrow$.

In this way we cleaned the surface from undesired functional groups.

Next, Fe powders (~80 nm) were pressed together with SiC nanostructures and sintered to produce a non-porous composite. Fe/SiC powders uniaxially compacted in a cylindrical mold (internal diameter of 15 mm, the height of the compacts 5-7 mm) at a pressure of up to 500 MPa, holding under pressure for 180 seconds.

Finally, Fe/SiC samples were sintered in a tube furnace. To achieve the lowest porosity, composites were sintered in H_2 atmosphere at 950°C for 2 hours with preheating the press from 700 to 950°C for 1 h.

3. Results and Discussion

TEM images for FeOOH particles are shown in Fig. 1. FeOOH particles showed the presence of aggregates with a length of ≤ 50 nm. S_{sp} for FeOOH is found to be 198 m^2/g from the nitrogen sorption experiment.

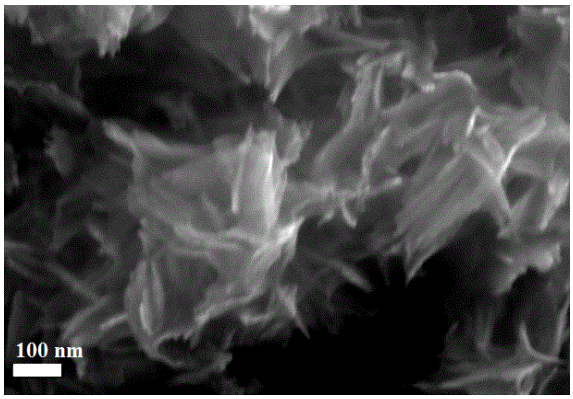

Fig. 1. Electronic microphotographs of FeOOH samples

Comparing the size of iron nanoparticles for FeOOH samples reduced at different temperatures, it follows that an increase in the reduction temperature of FeOOH samples from 400 to 550°C leads to an increase in the size of metallic iron particles.

The effect of reduction conditions on the phase composition, structure, and dispersion of resulting Fe powder was studied. Analysis of Fe powders by Mössbauer spectroscopy after reduction for 90 minutes at a temperature of 400°C and after reduction for 60 minutes in the temperature range of 450-550°C, showed that the samples contain only α-Fe (Fig. 2).

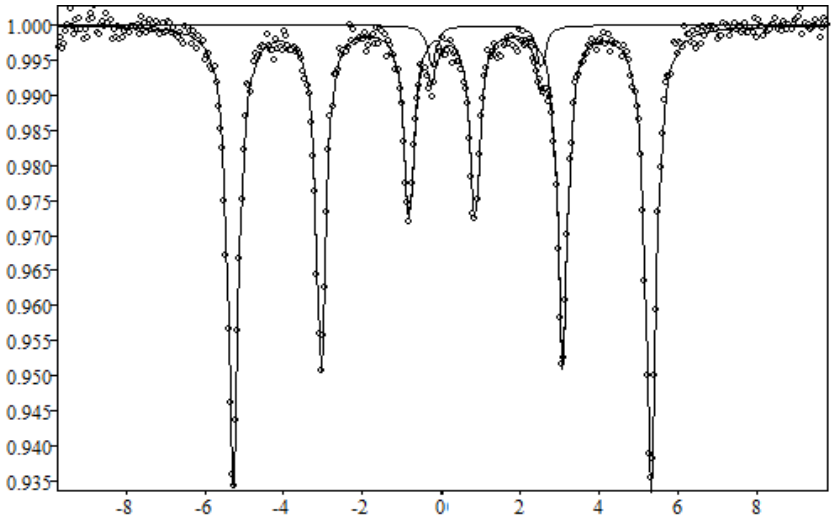

Sextets

#	G(Lorentz.)	A1(r.un.)	A2(r.un.)	A3(r.un.)	Γ1(mm/s)	Γ2(mm/s)	Γ3(mm/s)	IS(mm/s)	QS(mm/s)	Heff(mm/s)	%
1	1.000+/- 0.000	-0.067+/- 0.001	-0.049+/- 0.001	-0.027+/- 0.001	0.322+/- 0.005	0.298+/- 0.007	0.307+/- 0.011	0.000+/- 0.001	-0.004+/- 0.002	32.904+/- 0.009	99.0

Fig. 2. Mössbauer spectrum of Fe sample obtained from FeOOH dried at 120°C and reduced by H_2 at 400°C

The experimental specific surface areas and the calculated average sizes of dispersed Fe particles are listed in Table 1. An increase of reduction temperature from 400 to 550°C leads to a decrease in S_{sp} of metallic Fe from 8.4 to 2 m^2/g. Further, FeOOH reduction at 400°C for 90 minutes was used for the experiments.

Table 1. Specific surface area and the average size of Fe particles after reduction at different temperatures

Starting material	S_{sp}, m^2/g	Reduction temperature, °C	S_{sp}, m^2/g	d_{av}, nm
FeOOH heated at 120°C	150	400	8.4	90
		450	6.6	115
		500	3.7	200
		550	2.1	380

To create a nanostructured material, it is necessary at the first stage to obtain a metal matrix with a certain porosity.

The pressure varied from 50 MPa to 300 MPa. The pressing time ranged from 30 seconds to tens of minutes. The loading and unloading time varied from seconds to minutes.

The following mode was selected to get a Fe matrix with residual porosity 20-30%. For Fe NPs, applying a pressure of 200 MPa for 60 seconds, holding under pressure for 180 seconds, unloading for 30 seconds, powder weight – 9 g. Residual porosity is required for surface chemical reactions on the pore surface of Fe NPs.

The synthesis of SiC nanostructures on the porous iron matrix surface. SiC nanostructures on the porous Fe matrix surface were ALD-synthesized based on a series of successive surface reactions with functional groups on the surface. An important feature of ALD nanolayers is the absence of nucleation under certain synthetic conditions, which allows tuning the functional properties of the product more finely.

The synthesis included the following sequence of operations:

1. Porous Fe particles (1 g) were exposed to CCl_4 vapors at 350°C to remove the oxide layer (reaction 1).

2. Chlorinated samples underwent direct treatment by vapors of silicon-containing CH_3SiH for attaching silicon-carbon groups to the Fe particles surface (reaction 3).

3. Alternatively, the chlorinated sample was first converted to methylated one by methane treatment at 500°C (reaction 2). After that, the methylated sample reacted with $Cl_2Si(CH_3)_2$ (reaction 4).

$$[Fe]_aH + CCl_4 \rightarrow Fe]_a–Cl + HCl\uparrow, \quad (1)$$

$$[Fe]_a–Cl + CH_4 \rightarrow [Fe]_a–CH_3 + HCl\uparrow, \quad (2)$$

$$[Fe]_a–Cl + CH_3SiH \rightarrow [Fe]_a–CH_2SiH + HCl\uparrow, \quad (3)$$

$$[Fe]_a–CH_3 + Cl_2Si(CH_3)_2 \rightarrow [Fe]_a–HC=Si(CH_3)_2 + 2HCl\uparrow, \quad (4)$$

$$Fe]_a–HC=Si(CH_3)_2 + Cl_2Si(CH_3)_2 \rightarrow [Fe]_a–HC=Si(CH_3)_2–HC=Si(CH_3)_2 + 2HCl. \quad (5)$$

Reaction (3) resulted in the substitution of Cl by silicon-carbon groups. Since methylsilane is thermally stable up to 400°C, this reaction was performed in the range of 300-400°C. However, in this range, the replacement of Cl with silicon-carbon groups was not effective enough – ca. 40% (according to the Cl content in the product).

At the same time, methylation (reaction 2) and subsequent reaction with $Cl_2Si(CH_3)_2$ is found to give almost 100% replacement.

Based on these results, we further used reaction (4). Chemical analysis of modified Fe suggested that the Si and Cl content reaches a maximum at 400°C. The amounts of reacting silicon and chlorine on the sample remain approximately constant, with the Cl/Si ratio 2.4–2.6. Above 450°C the silicon content significantly decreases. Further increase of SiC nanolayer thickness is performed using reaction (5).

The reaction product comprises the Fe particles surface with silicon-carbon tails $HC=Si(CH_3)_2$ covalently bound to surface $–CH_3$ groups.

As a result of this work, Fe/SiC samples with varied SiC content were synthesized (Table 3).

Table 3. Composition of Fe/SiC samples

Sample No.	Cycles number	SiC content (wt%)	Sample composition
1	-	-	100% Fe
2	1	1.5	95.5% Fe + 1.5% SiC
3	2	3	97% Fe + 3% SiC
4	5	8.5	91.5% Fe + 8.5% SiC
5	10	15.5	84.5% Fe+ 15.5% SiC
6	16	25.5	74.5% Fe + 25.5 % SiC

Figure 3 shows the XRD pattern of sample No. 6 (SiC content 25.5 wt. %) that confirms the presence of α-Fe and SiC peaks.

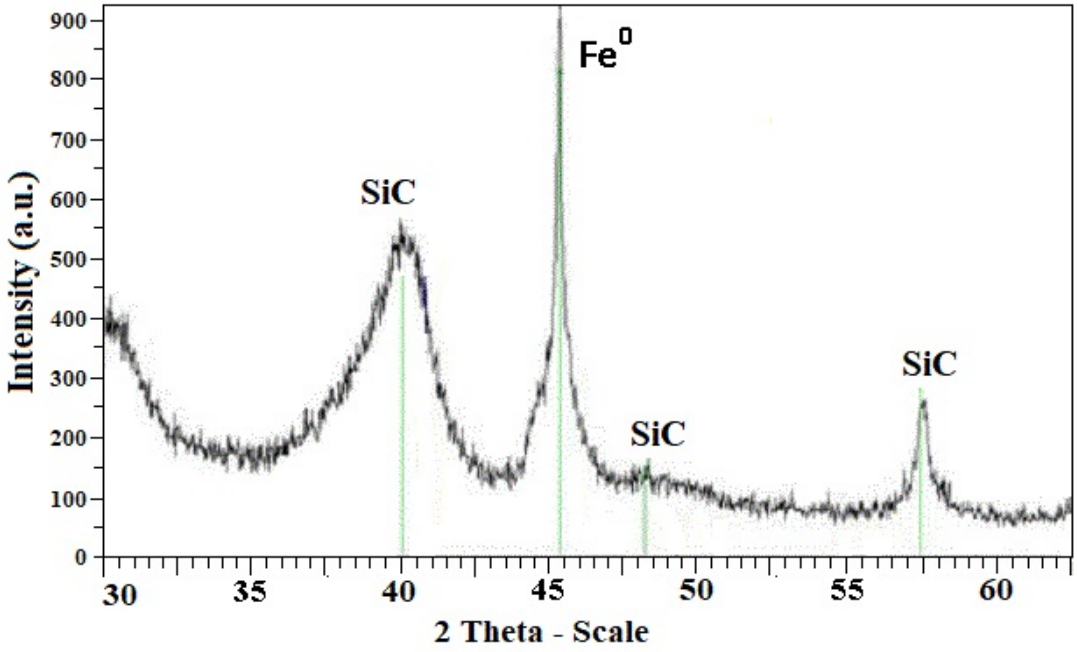

Fig. 3. XRD pattern of a Fe/SiC (25.5 wt%) sample after heating at 900°C

It is found that in the range of 700-800°C, SiC is in a partially amorphous state, while higher heating temperatures (900°C and more) leads to the formation of polycrystalline SiC. Based on XRD data, the average size of SiC crystallites after heating at 700-800°C is found to be ~2 nm, and at 900°C is ~6 nm.

Pressing and sintering of iron coated with hardening SiC nanostructures. Bulk nanocrystalline materials are of high interest because their structural and functional properties differ significantly from those of coarse-grained analogues [9,19].

Nanocrystalline materials are usually obtained by powder metallurgy, crystallization from an amorphous state, and severe plastic deformation. Features of nanocrystalline materials (grain size, a significant amount of interfaces, porosity, and other structural defects) depend on the preparation methods and have a significant impact on their properties.

The optimal conditions to achieve the best strength of non-porous compacts were analyzed, namely, the temperature and duration of sintering and pressing, intermediate temperature exposures, and the sintering medium (argon or hydrogen).

The pressure of 0.05 to 1.1 GPa was applied. A further increase in pressure does not lead to a significant increase in the compact density. At pressures of up to 0.5 GPa, the nanopowders compacted much less intensely than coarse particles. The loading time was varied from 1 to 23 minutes, the exposure duration under load ranged from 1 to 3 minutes, the duration of unloading was 2-4 minutes. The results of powder pressing show that loading for more than 15 minutes leads to the absence of cracks in the samples. Increasing the holding time under load from 1 to 3 minutes also leads to similar results.

To achieve the lowest porosity, compacts must be sintered in H_2 at 950°C for 2 hours with preheating of the press from 700 to 950°C for 1 h. This mode of sintering allowed to increase the density of the bulk sample (porosity is reduced to 5%). Sintering at a temperature above 1000°C did not improve the residual sample porosity.

Figure 4 depicts the nanowire formation on the α-Fe NPs surface. A SiC nanolayer of a predetermined thickness is formed on the surface of α-Fe nanoparticles. During the pressing and sintering stages, the pore walls of α-Fe NPs with a SiC nanolayer move towards each other. As a result, the SiC nanolayers are combined, and finally, a SiC nanowire is formed that permeates the entire α-Fe volume as a "frame within a frame" structure.

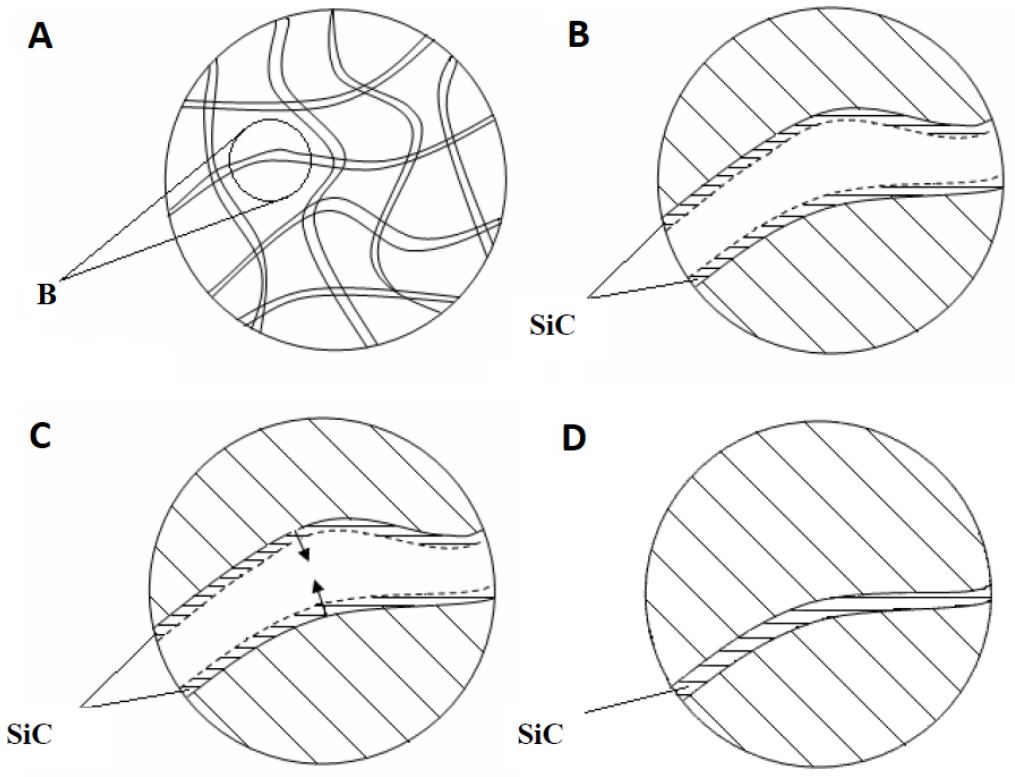

Fig. 4. Formation of the silicon carbide nanowires in the bulk nanocomposite on α-Fe: a) initial α-Fe with selected pore segment designated as B; b) pore segment on the walls of which the SiC nanolayer grows; c) SiC layers shift during pressing; d) merged SiC in the pore after compaction and sintering

Strength properties of metallic composites based on iron and silicon carbide strengthening nanomodifiers (Fe/SiC). The mechanical properties of nanomaterials depend significantly on the grain size. At the big grain sizes, an increase of the strength and hardness with decreasing grain size is due to the appearance of additional grain boundaries that are obstacles to dislocation motion. For small nanoscale grains, a strength increase is due to the low density of existing dislocations and the difficulty of new dislocations formation.

Strength data of Fe/SiC samples are presented in Fig. 5. For comparison, also the strength properties of the best grades of steel according to [20] are shown.

The ultimate strength of the obtained Fe/SiC composites is comparable to the properties of the best grades of steel, which contain a high percentage of alloying additives. Thus, it is evident that the formation of Fe/SiC composite using the surface structuring is a promising tool for obtaining new-generation composites.

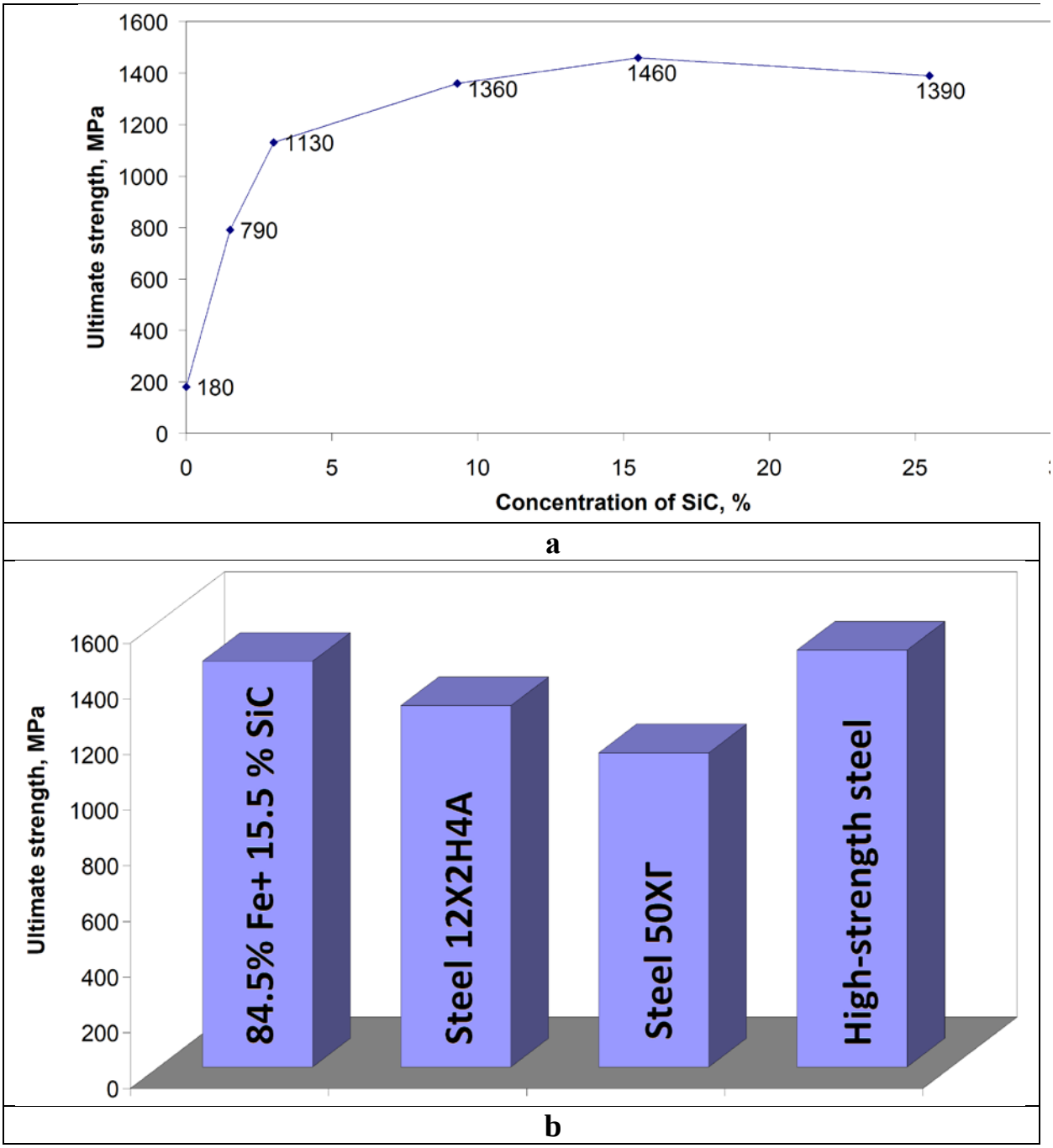

Fig. 5. The ultimate strength of a) Fe-based composites with SiC dispersed phase (this work); b) known steels in comparison with best sample composite

4. Conclusion

The authors offered the structuration of an iron-based metal matrix with carbide nanolayers, which results the composite with a "frame within a frame" structure. A synthesis has been developed of SiC nanolayers on the porous surface of Fe matrix during sequential chemisorption of CH_4 and $Cl_2Si(CH_3)_2$ molecules from the gas phase.

The conditions are established for pressing and sintering a Fe bulk material with nano-silicon carbide to obtain a composite with minimal residual porosity and improved strength.

The ways of adjustment of metal materials strength using structuring the metal matrix (on the example of iron) with SiC are discussed.

The proposed approach can also be used to create analogous composites based on an

aluminum frame with improved mechanical properties and is implemented via a nanosized material with a high degree of uniformity.

Acknowledgments. *The research was carried out on the basis of the Scientific Park of Saint Petersburg State University: RC "Innovative technologies of composite nanomaterials", RC "X-ray Diffraction research methods", an Interdisciplinary resource center in the field of "Nanotechnology". The work is financially supported by the Russian Science Foundation (Grant No. 20-11-20083).*

References

[1] Matthews FL, Rawlings RD. *Composite Materials: Engineering and Science*. Elsevier; 1999.

[2] Zemtsova EG, Monin AV, Smirnov VM, Semenov BN, Morozov NF. Synthesis of ceramic composites using three-dimensional nanostructuring (reinforcement) of alumina matrix with TiN and SiC nanostructures and study of their mechanical properties. *Physical Mesomechanics.* 2017;20(4): 438-446.

[3] Panin VE, Panin AV, Elsukova TF, Popkova YF. Fundamental role of curvature of the crystal structure in plasticity and strength of solids. *Physical Mesomechanics.* 2015;18(2): 89-99.

[4] Morozov NF, Tovstik PE. Chessboard-like buckling modes of compressed materials. *Doklady Physics.* 2012;57(3): 131-135.

[5] Hotta M, Kita H, Hojo J. Nanostructured silicon carbide ceramics fabricated through liquid-phase sintering by spark plasma sintering. *Journal of the Ceramic Society Japan*. 2011;119(1386): 129-132.

[6] Rosso M. Ceramic and metal matrix composites: Routes and properties. *J. Mater. Proc. Tech.* 2006;175(1-3): 364-375.

[7] Tolochko OV, Koltsova OT, Bobrynina EV, Rudskoy AI, Zemtsova EG, Kirichenko SO, Smirnov VM. Conditions for production of composite material based on aluminum and carbon nanofibers and its physic-mechanical properties. *Nanomaterials.* 2019;9(4): 550.

[8] Smirnov VM. Nanoscaled structuring as a way to constructing new solid substances and materials. *Russian Journal of General Chemistry.* 2002;72(4): 633-650.

[9] Zemtsova EG, Monin AV, Smirnov VM, Semenov BN, Morozov NF. Formation and mechanical properties of alumina ceramics based on Al_2O_3 micro- and nanoparticles. *Physical Mesomechanics.* 2015;18(2): 134-138.

[10] Monin AV, Zemtsova EG, Shveikina NB, Smirnov VM. Features of phase transitions upon the thermal treatment of Al_2O_3 nanoparticles. *Nanotechnologies in Russia.* 2012;7(3-4): 152-155.

[11] Nazarov DV, Smirnov VM, Zemtsova EG, Shevtsov MA, Valiev RZ. Enhanced osseointegrative properties of ultra-fine-grained titanium grained implants modified by chemical etching and atomic layer deposition. *ACS Biomaterials Science and Engineering.* 2018;4(9): 3268-3281.

[12] George SM. Atomic layer deposition: an overview. *Chemical Reviews.* 2010;110(1): 111-131.

[13] Smirnov VM, Zemtsova EG, Morozov PE. Forced organization of magnetic quasi-one-dimensional iron-organic nanostructures on inorganic matrices. *Reviews on Advanced Materials Science.* 2009;21(2): 205-210.

[14] Smirnov VM, Zemtsova EG, Ivanov EB, Semenov VG, Murin IV. Mössbauer and magneto-chemical study of solids formed by surface chemical reaction of OH-silica groups with iron diacetylacetonato chloride $(C_5H_7O_2)_2FeCl$. *Applied Surface Science.* 2002;195(1-4): 89-92.

[15] Ermakova LE, Sidorova MP, Smirnov VM. Isoelectric point of silicon oxide particles coated by monolayers of oxides of titanium and aluminum. *Koll. Zh.* 1997;59(4): 563-565
[16] Zemtsova EG, Arbenin AY, Valiev RZ, Semenov VG, Smirnov VM. Two-level micro-to-nanoscale hierarchical TiO_2 nanolayers on titanium surface. *Materials.* 2016;9(12): 1010.
[17] Smirnov VM, Povarov VG, Voronkov GP, Gittsovich VN, Sinel'nikov BM. Solid-state water-mediated transport reduction of nanostructured iron oxides. *Journal of Nanoparticle Research*. 2001;3(1): 83-89.
[18] Smirnov VM, Bobrysheva NP, Osmolowsky MG, Semenov VG, Murin IV. Surface magnetic ordering of Fe-O and Ti-O groups disposed on diamagnetic support. *Surface Review and Letters.* 2001;8(3-4): 295-302.
[19] Ataee-Esfahani H, Vaezi MR, Nikzad L, Yazdani B, Sadrnezhaad SK. Influence of SiC nanoparticles and saccharin on the structure and properties of electrodeposited Ni–Fe/SiC nanocomposite coatings. *Journal of Alloys and Compounds.* 2009;484(1-2): 540-544.
[20] Solntsev YP, Pryakhin EI. *Material Science.* St. Petersburg: Himizdat; 2007.